Crystal growth, optical, thermal, dielectric and mechanical studies on a nonlinear organic optical material: guanidinium fumarate dihydrate (GFDH) single crystal

K. Krishnaraj[1] and P. Praveen Kumar[1,*] (iD)

[1] *Department of Physics, Presidency College, Chennai, Tamil Nadu 600 005, India*

ABSTRACT

Guanidinium fumarate dihydrate (GFDH), an organic material was grown by slow evaporation method at room temperature. The monoclinic system of the GFDH crystal was affirmed by single XRD analysis and its space group was determined to be $P2_1/n$. The quality of the grown optical GFDH crystal was confirmed with HRXRD analysis. The molecular structure of the GFDH crystal was studied by FT-IR spectroscopy. UV–Vis study demonstrates the lower cut-off wavelength (320 nm) and higher optical transparency of the GFDH crystal. The Meyer's index value ($n = 1.23$) of the GFDH crystal shows that the GFDH crystal belongs to hard material category. Information regarding the thermal stability and melting point were rendered from the TG–DTA thermal studies. Dielectric studies were performed to understand the various polarization mechanisms at different temperatures. The GFDH crystal exhibits high third-order non-linear optical properties and optical limiting properties and that was analyzed by the Z-scan technique.

1 Introduction

In recent decades, search of potential organic nonlinear optical materials with fast optical response are highly important for various applications like optical limiting, medical imaging, harmonic generation, optical parametric oscillation and the fabrication of optoelectronic devices [1, 2]. The inorganic crystals have high mechanical strength and thermal stability but low optical nonlinearity. Organic materials are under investigation because of its flexibility, high nonlinearities and they can be used to design new novel materials. The presence of π-electron conjugated systems in organic materials makes the material polarisable, and they are suitable for NLO applications.

Currently, fumaric acid plays an important role in the formation of good quality crystals. Similar to the other binary carboxylic acids, it tends to form infinite

---

Address correspondence to E-mail: ppkpresidency@gmail.com

🖉 Springer

chains arranged in a nearly coplanar manner by pairs of strong O–H…O hydrogen bonds.

Guanidinium is a strong base and simple organic material and can easily react with the majority of the organic acids and gives the good crystalline product because of its structures is related to those of amides and proteins and its specific planar configuration makes the cation as a potential H-donor in hydrogen bonds interaction [3]. Guanidine are used to manufacture of plastics, photo chemicals, resins and disinfectant in industry because of its structure containing nitrogens and N=C solid bond.

Guanidinium-based organic compounds such as guanidinium cinnamate [4], guanidinium tartrate hydrate [5], guanidinium 4-aminobenzoate [6], guanidinium perchlorate [7] and aminoguanidinium (1+) hydrogen L-tartrate monohydrate, have been reported [8]. The structure of the guanidinium fumarate dihydrate (GFDH) was studied and already reported [9].

In the present work, GFDH crystal was grown by slow evaporation solution growth technique. The grown GFDH single crystal is characterized by single XRD and the crystalline perfection of the GFDH crystal is obtained by HRXRD. The various functional groups of title compound are confirmed by FT-IR analysis. The optical absorption spectrum of GFDH crystal shows that the lower cut-off wavelength is at 320 nm. Microhardness, dielectric, third-order optical properties have been investigated for GFDH crystal.

2 Experimental procedure

2.1 Material synthesis

Analytical reagent (AR) grade guanidinium carbonate and fumaric acid salt was dissolved in water and the saturated solution was prepared at room temperature. The starting material was synthesized in the stoichiometric 1:1 ratio and the reaction scheme is,

$$C_3H_{12}N_6O_3 + C_4H_4O_4 + H_2O$$
$$\rightarrow [CN_3H_6]_2 \cdot C_4H_2O_4 \cdot 2H_2O + CO_2 \uparrow.$$
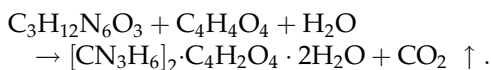
The transparency of the crystal was improved by consecutive recrystallization process. Optically good transparent GFDH single crystal is obtained by slow evaporation solution technique. The GFDH material with good shape and dimension of $17 \times 16 \times 6$ mm^3

was grown within 30 days and it is displayed in Fig. 1a.

2.2 Solubility studies

The solubility process is important for growing good quality crystals. The solubility study of GFDH crystal was carried out at different temperatures ranging from 30 to 50 °C with an interval of 5 °C using a constant temperature bath with the accuracy of ± 0.01 °C. Small amount of compound was dissolved in 100 ml water and maintained in constant temperature bath at 30 °C. Good solubility of the title compound was obtained by continuous stirring using magnetic stirrer at different temperatures. The solubility curve of GFDH crystal is depicted in Fig. 1b. It can be seen from the figure that the solubility increases with the increase in temperatures, which indicates that the GFDH has a positive solubility.

2.3 Measurement techniques

Single XRD study was done for GFDH using Bruker kappa APEX II CCD diffractometer instrument with Mo Kα ($\lambda = 0.71073$ Å) radiation. The fine powder of grown GFDH crystal was analyzed using Bruker D8 advanced powder X-ray diffractometer with the Cu Kα radiation ($\lambda = 1.5407$ Å) to check the crystalline nature and quality. The crystallinity of GFDH was analyzed using high-resolution X-ray diffraction (Model: PANalytical X'Pert PRO MRD). The Fourier transform infrared (FTIR) spectrum of title
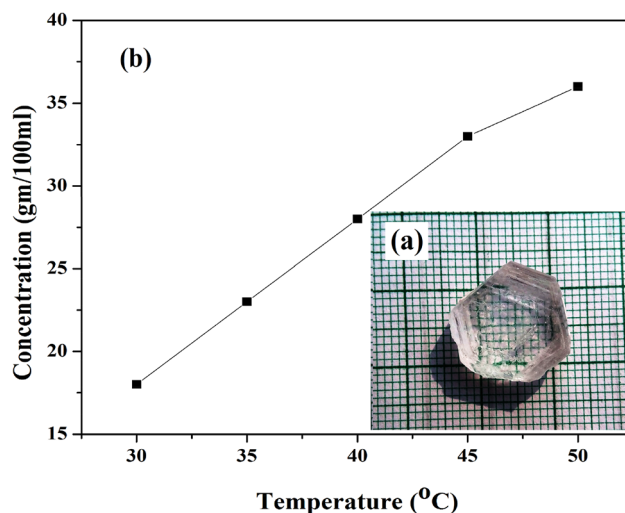
Fig. 1 a GFDH single crystal and b solubility of GFDH in water solvent

compound was recorded in the range of 4000–400 cm^{-1} using a Perkin-Elmer spectrometer. The optical absorption behavior of the grown guanidinium fumarate dihydrate crystal was recorded in the range 200–800 nm using a Varian Cary 5E UV–Vis spectrophotometer. Thermal studies (TG/DTA) were performed on GFDH crystal using TGA Q 500 V20 instrument. Dielectric analysis of the grown GFDH single crystal was analyzed using Hioki 3532-50 LCR Hitester instrument. Leitz Wetzlar Vickers microhardness tester was employed to test the mechanical hardness of the grown crystal. Z-scan studies were performed on the crystal using Nd:YAG laser of wavelength 532 nm to estimate the third-order nonlinear optical susceptibility [$\chi^{(3)}$] and to understand the optical limiting phenomena.

3 Results and discussion

3.1 Single crystal X-ray diffraction study

Single XRD study confirmed that the title compound crystallizes in monoclinic crystal system with the space group $P2_1/n$. The obtained lattice parameter values are $a = 7.82$ Å, $b = 8.92$ Å, $c = 9.59$ Å, $\alpha = \gamma = 90°$, $\beta = 93.27°$ and $V = 668$ Å^3 and are shown in Table 1. These crystallographic parameters are well matched with the reported values [9].

3.2 Powder XRD studies

The formation of crystal system and crystallinity of the GFDH compound were analyzed through powder X-ray diffraction (PXRD) study. The recorded PXRD pattern of GFDH is shown in Fig. 2a. The

Table 1 Lattice parameters of guanidinium fumarate dihydrate single crystal

| Cell parameters	Present work	Reported value [9]
a (Å)	7.82	7.86
b (Å)	8.92	8.98
c (Å)	9.59	9.64
$\alpha^O = \gamma^O$	90	90
β^O	93.27	93.19
v (Å^3)	668	680
Space group	$P2_1/n$	$P2_1/n$
Crystal system	Monoclinic	Monoclinic

experimental XRD pattern is well matched with the simulated XRD pattern and is depicted in Fig. 2b. A sharp well defined peak observed at 23° of the (120) plane confirm the crystallinity of the synthesized material [10].

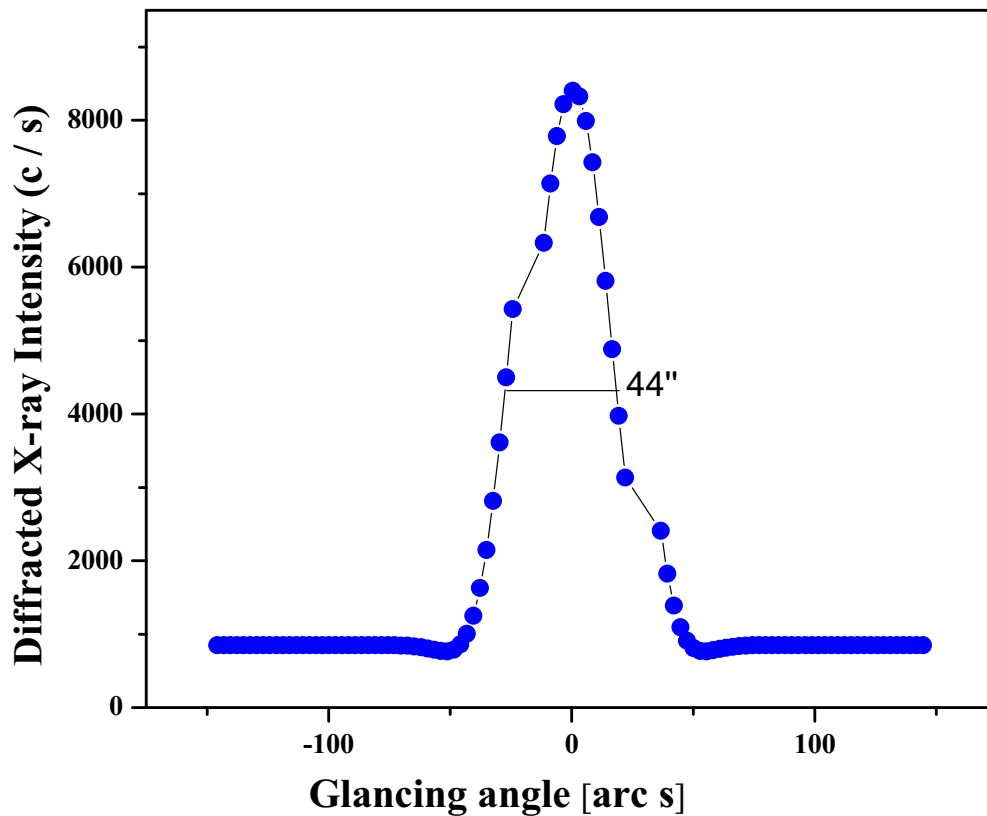### 3.3 High-resolution X-ray diffraction (HRXRD)

HRXRD study was used on the grown GFDH single crystal to understand the crystallinity. The HRXRD curve is shown in Fig. 3. The diffraction curve contains only one peak without any satellite peaks; this clearly indicates that the grown GFDH crystal does not contain any internal structural grain boundaries and the absence of impurities at macroscopic level. From the figure, it is noticed that the full width half maximum diffraction of the curve of GFDH grown crystal is 44″ which is somewhat more than that predictable value from the plane wave theory and it reveals the presence of low point defects and good quality. Therefore, GFDH single crystal can be used for optoelectronic applications.

3.4 Fourier transform infrared (FTIR) analysis

Infrared spectroscopy is used to identify the functional groups present in the synthesized material. The FT-IR spectrum of GFDH crystal is recorded and is
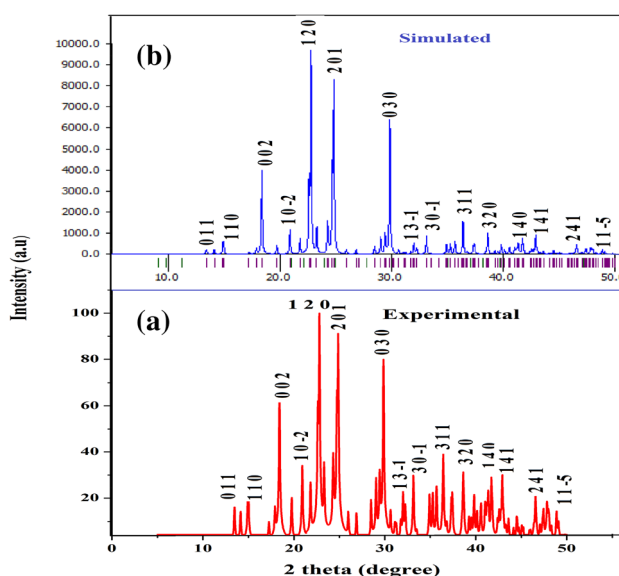

Fig. 2 Powder XRD patterns of GFDH: **a** experimental and **b** simulated

Fig. 3 High-resolution X-ray diffraction curve recorded for a typical GFDH crystal

shown in Fig. 4. The absorption peaks observed at 3361 cm^{-1} are assigned to O–H stretching vibration. The peak at 3019 cm^{-1} is due to the presence of strong aromatic C–H stretching vibration. The peak at 1643 cm^{-1} is due to presence of C=C stretching vibration. The peak at 1516 cm^{-1} is assigned for N–O

asymmetric stretching vibration. The peaks at 1194 cm^{-1} and 1144 cm^{-1} indicate C–N stretching vibrations. The peak at 952 and 802 cm^{-1} is assigned to the presence of C–H bending mode. The peak at 670 cm^{-1} is assigned to the presence of N–H stretching mode.
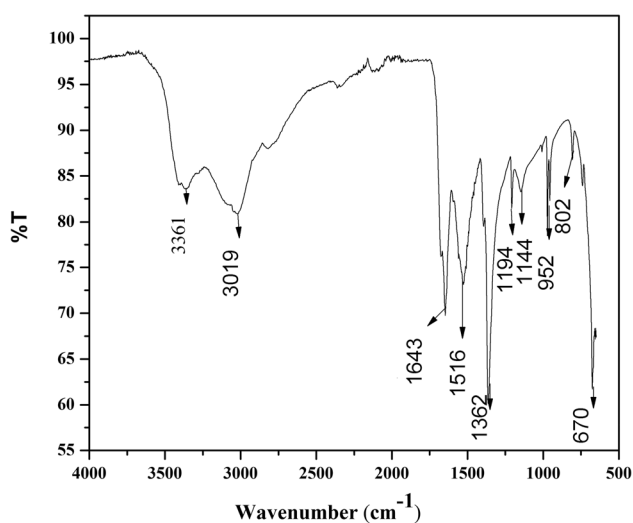
### 3.5 UV–Vis spectral analysis

UV–Vis study is an important tool to provide information regarding, optical transparency, bandgap as well as the process of electronic transition in the solid molecule [11]. The spectrum of GFDH material was carried out in the range 200–800 nm were displayed in Fig. 5a. GFDH is a colorless crystal that shows low absorption in the entire visible region which is a most desirable property for NLO applications. From the spectrum, it was found that the lower cut-off wavelength (λ) of the GFDH material is 320 nm. The α value was evaluated using the relation:

$$\alpha = \frac{2.3026 \log\left(\frac{1}{T}\right)}{t}, \tag{1}$$

where α is the linear optical absorption coefficient, T

Fig. 4 FTIR spectrum of GFDH crystal
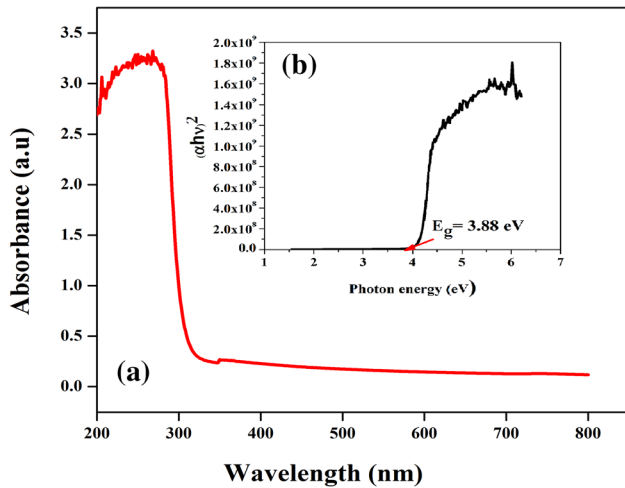
Fig. 5 a Optical absorption spectrum and **b** optical bandgap energy of GFDH

is the transmittance (%) and the thickness (t) of the title compound. The absorption coefficient (α) near the absorption peak was assessed using the formula:

$$(\alpha h v)^2 = A(vh - E_g)^m, \tag{2}$$

where v is the frequency of the incident radiation, A is the constant and m is the integer value indicating the indirect (2) and direct (1/2) optical transitions [12]. As this crystal corresponding to a direct transition, the bandgap of crystal was calculated plot between $(\alpha h v)^2$ versus $h v$ as shown in Fig. 5b. The E_g value calculated using the below formula:

$$E_g = \frac{hc}{\lambda_e} \text{ (eV)}, \tag{3}$$

where c is the velocity of light in vacuum, h is the Planck's constant and λ_e is the lower cut-off wavelength of the GFDH crystal. The direct optical bandgap (E_g) of the GFDH crystal is found to be 3.88 eV. The optical bandgap E_g of the GFDH crystal shows that the crystal has good optical transmittance. Therefore, it may be a suitable candidate for optical switching and optoelectronic applications [13, 14].

3.6 Thermal studies

Thermal stability, decomposition and melting point of the grown GFDH sample have studied from thermogravimetric (TG) and differential thermal analysis (TG–DTA) [15]. 1.9 mg of crystalline powder has taken in an alumina crucible. Nitrogen gas has allowed entering the furnace to maintain a stable inert nitrogen atmosphere. The sample has heated in

the temperature range of 35–500 °C with the heating rate of 20 °C/min. TGA–DTA curves of GFDH material are shown in Fig. 6. The TG curve shows two stage weight losses in the GFDH material. The first weight loss shows in the temperature range from 35 up to 105 °C due to loss of water molecules in the crystal lattice. After the dehydration, the GFDH compound is almost intact up to 248 °C, followed which it decomposition. This confirms that before this temperature there was no endothermic or exothermic transition. The second major weight loss pattern occurred between 248 and 500 °C, This weight loss is may be to the release of CO_2, CO, NO_2, NH_3 molecules.

DTA was also conducted between 35 and 500 °C. The resulting curve is illustrated in Fig. 6. There was one sharp endothermic peak at 249 °C which represent the melting of the GFDH crystal. The sharp endothermic peak found matching with the second weight loss in TGA curve. A sharp endothermic peak at 249 °C reveals excellent phase transformation.

3.7 Dielectric studies

The information about changes of structural, behavior of defect, molecular anisotropy and optical properties within the crystalline materials can be easily known by the dielectric studies. With dielectric studies, polarizability can be detected within nonlinear optical materials [16, 17]. The dielectric constant (ε') and dielectric loss (ε'') with log of frequencies were determined for different temperatures (40–70 °C). The ε' was determined from Eq. 4:
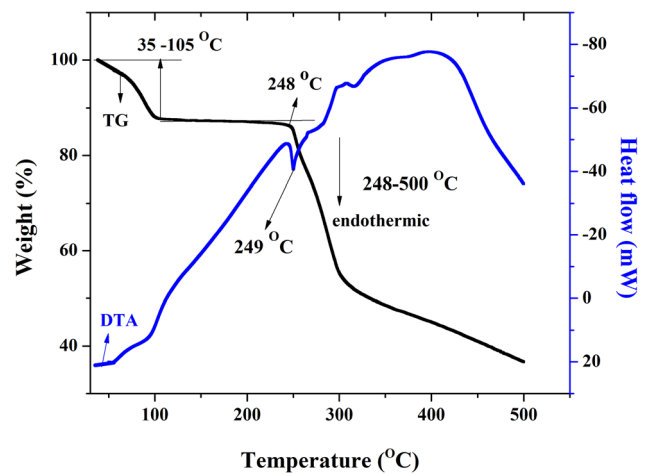
Fig. 6 TG and DTA of GFDH

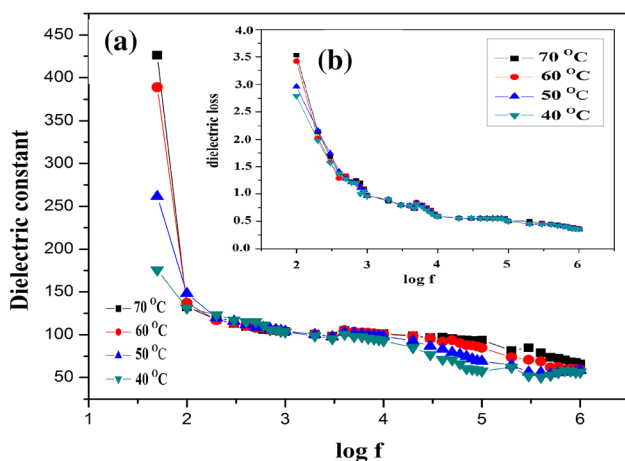$$\varepsilon' = \frac{Ct}{A\varepsilon_0}, \tag{4}$$

where C is the capacitance, ε_0 is the permittivity of free space. The dielectric loss ε'' was calculated for GFDH material using the equation,

$$\varepsilon'' = D\varepsilon', \tag{5}$$

where D is the dissipation factor. The variation of dielectric constant of the crystal with the log of frequency for different temperatures has depicted in Fig. 7a. From the figure, the ε' decreases with increase frequency. The high value of ε' at low frequencies, may be due to the space charge, orientation, ionic and dipole polarizations. Space charge polarization is usually may be active at high temperatures and high ε' at lower frequencies and exposed the purity and perfection of the materials [18, 19]. Figure 7b represents the variation of ε'' with log of frequency for various temperatures. The ε'' is low with high frequency for the crystal suggests that it has improved good optical quality with fewer defects. Hence this GFDH crystal is suitable for nonlinear optical applications [20, 21].

3.7.1 Estimation of solid-state parameters of GFDH single crystal

Electronic polarizability (α) can be estimated using two approaches such as Penn gap analysis and Clausius–Mossotti relation. To perform the computational process, it is necessary to first determine certain quantities such as valence electron plasma energy, Penn gap energy and Fermi energy. This

solid-state parameter has estimated based on the molecular formula of the GFDH single crystal. The molecular weight $M = 680.4$ g/mol, the density (ρ) of the GFDH single crystal: 1.32 Mg/m³. The total number of valence electrons (Z) of the $C_6H_{18}N_6O_6$ crystal has obtained as $Z = (6 \times Z_C) + (18 \times Z_H) + (6 \times Z_N) + (6 \times Z_O) = 144$. At high frequency (5 MHz), the ε_∞ has estimated to be 14.18.

The valence electron plasma energy ($\hbar\omega_p$) can be determined using following formula:

$$\hbar\omega_p = 28.8 \left(\frac{\rho \cdot Z}{M} \right)^{\frac{1}{2}}. \tag{6}$$

Using the plasma energy ($\hbar\omega_p$), the Penn gap (E_P) and the Fermi energy (E_F) has calculated from the following equations:

$$E_P = \frac{\hbar\omega_p}{(\varepsilon_\infty - 1)^{\frac{1}{2}}}, \tag{7}$$

$$E_F = 0.2948(\hbar\omega_p)^{\frac{4}{3}}. \tag{8}$$

S_O is a constant for a specific compound and it has obtained using the formula:

$$S_O = 1 - \left[\frac{E_P}{4E_F} \right] + \frac{1}{3} \left[\frac{E_P}{4E_F} \right]. \tag{9}$$

The α values of the GFDH crystal has calculated from the Penn gap relation:

$$\alpha = \left[\frac{S_O(\hbar\omega_p)^2}{S_O(\hbar\omega_p)^2 + 3E_P^2} \right] \times \frac{M}{\rho} \times 0.396 \times 10^{-24} \text{ cm}^3. \tag{10}$$

The α values has also confirmed using the Clausius–Mossotti approach as:

$$\alpha = \frac{3M}{4\pi\rho N_a} \left[\frac{\varepsilon_\infty - 1}{\varepsilon_\infty + 2} \right] \text{ cm}^3. \tag{11}$$

The estimated values of the E_P, E_F, α and S_O of the GFDH compared to the standard KDP are listed in Table 2. The values of GFDH single crystal is high compare to KDP material.

3.8 Microhardness analysis

Microhardness study helps to understand types of mechanical strength of a single crystal. The microhardness has been studied different load from 10 to 60 g for an indentation time of 5 s. The Vickers

Fig. 7 **a** Dielectric constant (ε_r) with log frequency and **b** dielectric loss with log frequency of GFDH

hardness number Hv was calculated using the equation:

$$Hv = 1.8544 \left(p/d^2 \right) \text{ kg/mm}^2, \tag{12}$$

where p is the applied load and d is the diagonal length. The graph plotted between to Hv and p is presented in Fig. 8a. From the plot has observed that the Hv decreases with the increase p and it is related to the indentation size effect (ISE). For above 60 g, cracks started increasing around the indentation mark. This may be the release of internal stress generated locally by indentation.

3.8.1 Analysis of Meyer's law

The simplest to describe the ISE is Meyer's law, the relation between the applied indentation load (p) and size of indentation (d) is given as follows,

$$p = A_1 d^n, \tag{13}$$

where n is the Meyer's index and A is the material constant. The value of n for normal indentation size effect (ISE) behavior is less than 2 ($n < 2$). Similarly, the reverse indentation size effect is expressed when the [RISE] behavior is greater than n value 2 ($n > 2$). The value of n can be evaluated from the Meyer's graph of log p vs log d. Figure 8b shows the plot between log p and log d. In this study, n found to be 1.23 (ISE) for GFDH. According to rule of Onitsch, for hard materials category the n is below 1.6 and for soft materials category greater than 1.6 [22, 23]. Therefore, GFDH belongs to hard material category, which may be caused by higher bonding forces between the atoms of the material.

3.8.2 Analysis of yield strength (σ_y)

The σ_y of the crystal can be estimated from the 'Hv' and depends on n value. For $n > 2$, the σ_y can be evaluated from Eq. 14:

$$\sigma_y = \left(\frac{Hv}{2.9} \right) [1 - (n-2)] \left\{ 12.5 \frac{n-2}{1-(n-2)} \right\}^{n-2}. \tag{14}$$

In the present study, n value is not greater than 2 ($n < 2$, 1.23), so the yield strength was estimated using the following expression [24]:

$$\sigma_y = \frac{Hv}{3}. \tag{15}$$

It is seen from Fig. 8c that the σ_y decreases also as p increases. The measured results are displayed in Table 3.

3.8.3 Analysis of elastic stiffness constant (C_{11})

The stiffness constant (C_{11}) for various loads has been estimated using Wooster's empirical equation [1]. It is presented an extensive idea about the high bonding forces between neighboring atoms in the material.

$$C_{11} = (Hv)^{\frac{7}{4}}. \tag{16}$$

It is seen from Fig. 8d that the C_{11} decreases also as p increases. The measured results have been displayed in Table 3.

3.9 Z-scan technique

The third-order nonlinear properties of the GFDH crystal were analyzed through Z-scan technique. The values of third-order nonlinear optical parameters like nonlinear refractive index (n_2), the nonlinear absorption coefficient (β) and the optical nonlinear susceptibility $\chi^{(3)}$ can only be estimated from the open and closed aperture Z-scan curves [25, 26]. In the open aperture mode, laser light coming from the crystal was collected directly using the photo detector along with a digital power meter.. The recorded GFDH crystal open aperture curve is depicted in Fig. 9a and it exhibits saturable absorption behavior. The recorded closed aperture curve of GFDH are displayed in Fig. 9b and it has concluded that the

Table 2 The electronic parameters estimated for BGTTH single crystal

Parameters	Present study	KDP values
Plasma energy (eV)	24.134	17.28
Penn gab (eV)	6.647	2.37
Fermi energy (eV)	20.555	12.02
Electronic polarizability α (cm^3) using Penn analysis	6.506×10^{-23}	2.14×10^{-23}
Electronic polarizability α (cm^3) using Clausius–Mossotti equation	6.620×10^{-23}	2.10×10^{-23}
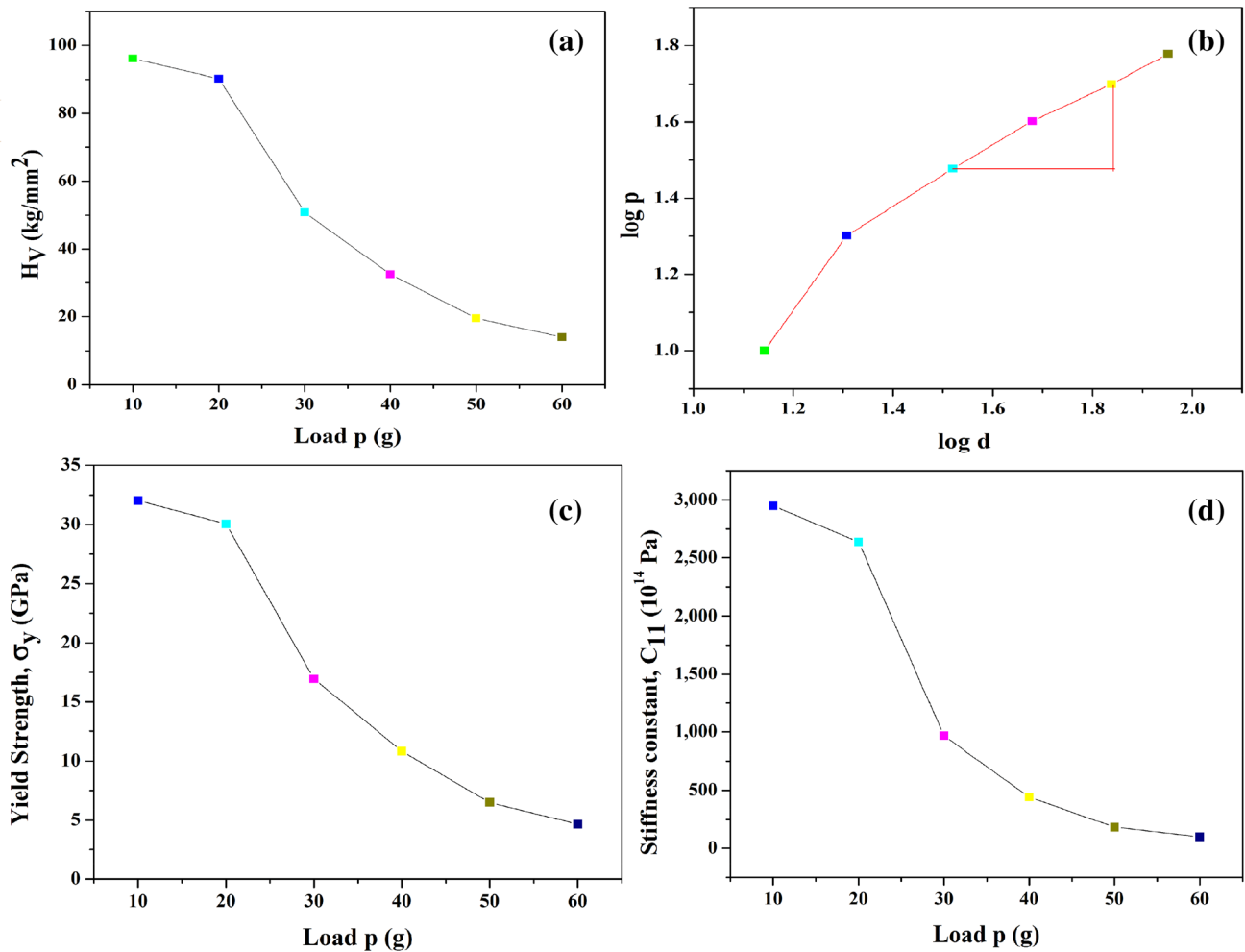
Fig. 8 **a** Plot of load p vs. Hv, **b** plot of log d vs. log p, **c** plot of load p vs. σ_y and **d** variation of load p vs. C_{11} of GFDH crystal

Table 3 Microhardness number (Hv), yield strength and stiffness constant values of GFDH material

| Load, p (g)	Hardness number, H_V (kg/mm^2)	Yield strength, σ_y (GPa)	Stiffness constant, $C_{11} \times 10^{14}$ (Pa)
10	96.11395	32.03798294	2950.368319
20	90.1738	30.057934	2638.703949
30	50.84138	16.94712562	968.0109744
40	32.50262	10.83420693	442.4428351
50	19.52796	6.509319182	181.4050776
60	13.92042	4.64014095	100.320976

crystal exhibits peak followed by a valley which is indicated that the nonlinear refractive index is negative sign, that is, strong self-defocusing behavior of the title compound.

The normalized peak and valley transmittances (ΔT_{P-V}) were determined using,

$$\Delta T_{P-V} = 0.406(1 - S)^{0.25}|\Delta_0|, \tag{17}$$

$$S = 1 - \exp\left(\frac{-2r_a^2}{\omega_a^2}\right). \tag{18}$$
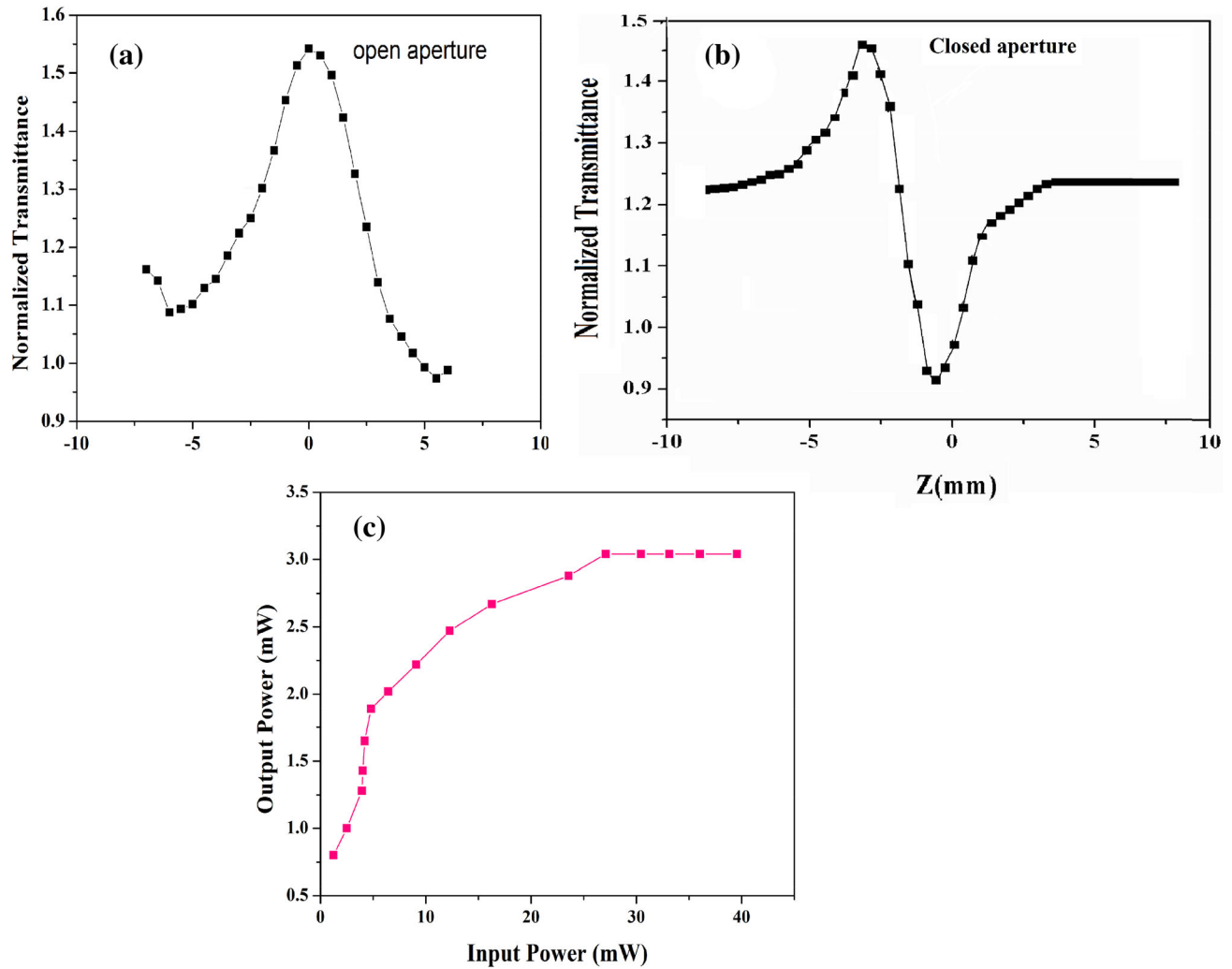
Fig. 9 **a** Z-scan plot for open aperture, **b** Z-scan plot for closed aperture and **c** optical limiting spectrum of GFDH crystal

The radius of aperture (r_a); the beam radius of aperture (ω_a). The n_2 was evaluated using the following formula [27]:

$$n_2 = \frac{\Delta\varphi_0}{\kappa L_{\text{eff}} I_0}. \tag{19}$$

The β was estimated using the below equation:

$$\beta = \frac{2\sqrt{2}\Delta T}{I_0 L_{\text{eff}}}, \tag{20}$$

where ΔT indicates the peak value at the open aperture plot. I_o indicates the input intensity of the incident beam and L_{eff} is presented by $[1 - \exp(-\alpha L)]/\alpha]$, here L indicates as thickness of the sample and α denotes as linear absorption coefficient.

$$\text{Re}\chi^{(3)} \text{ (esu)} = \frac{10^{-4}(\varepsilon_0 n_2 c^2 n_0^2)}{\pi} \text{ cm}^2/\text{W} \tag{21}$$

and

$$\text{Im}\chi^{(3)} \text{ (esu)} = \frac{10^{-2}(\varepsilon_0 \lambda \beta c^2 n_0^2)}{4\pi^2} \text{ cm/W}. \tag{22}$$

From Eqs. (21) and (22), were obtained the real and imaginary part of third-order NLO susceptibility [28]. The permittivity of free space ($\varepsilon_0 = 8.854 \times 10^{-12}$ F/m); the velocity of light in vacuum ($c = 3 \times 10^8$ m/s); the $\chi^{(3)}$ of the GFDH material was evaluated using the following formula:

$$\chi^{(3)} = \sqrt{(\text{Re}\chi^{(3)})^2 + (\text{Im}\chi^{(3)})^2}. \tag{23}$$

The estimated third-order nonlinear optical parameter of the GFDH crystal is listed in Table 4.

Table 4 Third-order nonlinear optical parameters of GFDH using Z-scan technique

Nonlinear refractive index (n_2)	-4.1243×10^{-8} (cm^2/W)
Nonlinear absorption coefficient (β)	0.6123×10^{-4} (cm/W)
Real part of the third-order susceptibility [Re$\chi^{(3)}$]	6.23145×10^{-6} (esu)
Imaginary part of the third-order susceptibility [Im$\chi^{(3)}$]	2.9411×10^{-6} (esu)
Third-order nonlinear optical susceptibility [$\chi^{(3)}$]	6.8906×10^{-6} (esu)

The negative refractive index value (-4.1243×10^{-8} cm^2/W) of the grown crystal represents the self-defocusing nature and the reverse saturable absorption which finds optical limiting applications [29]. The grown crystal possesses a high value of $\chi^{(3)}$ (6.8906×10^{-6} esu). This could be due to the availability of fast π-electron cloud movement which is responsible for higher molecular polarizability [30]. Thus the GFDH material can be used for photo sensors and nonlinear optical applications.

3.10 Optical limiting studies

The optical limiting effect is a nonlinear optical process [nonlinear absorption (NA) and nonlinear refraction (NR)] in which the transmitted signal from the sample increases with input signal intensity and remains constant at threshold intensity. The optical limiting process can be achieved by various NLO mechanisms, including induced scattering, two-photon absorption, self-defocusing and photo-refraction in NLO media [31]. The optical limiting behavior of GFDH material is depicted in Fig. 9c. From the figure, it is noted that the output power intensity reaches saturated point called as limiting amplitude of the GFDH single crystal. The limiting threshold for saturation and output clamping values were found to be 27.14 mW and 3.02 mW, respectively. Therefore, the grown GFDH single crystal is used to protect the human eyes and optical sensor systems, because of its good optical limiting applications [32].

4 Conclusion

Third-order nonlinear optical single crystal of guanidinium fumarate dihydrate single crystal with $17 \times 16 \times 6$ mm^3 dimension has grown by slow evaporation solution method. The grown GFDH single crystal has good solubility in water. It has been found that the grown GFDH single crystal belongs to the monoclinic system with the $P2_1/n$ space group by the single X-ray diffraction studies. The crystalline planes and their crystallinity has detected by the powder XRD measurement. HRXRD confirms the quality of the grown crystal. FT-IR study confirms the molecular structure of the titled material. UV–Vis spectral analysis shows that the lower cut-off wavelength of the grown crystal is 320 nm. Bandgap energy was found to be 3.88 eV. The thermal stability of the GFDH single crystal has studied by TG–DTA analysis. The dielectric studies revealed that the GFDH crystal exhibit good dielectric behavior. The Vicker's microhardness measurements reveal that GFDH crystal belongs to hard material category. The grown crystal show negative refractive index value (-4.1243×10^{-8} cm^2/W) as well as high third-order nonlinear optical susceptibility value (6.8906×10^{-6} esu). Also, the limiting threshold of saturation (27.14 mW) and output clamping value (3.02 mW) of the grown crystal find potential application in the field of eye surgery and optical sensor devices.

References

1. N. Khan, N. Vijayan, K. Shandilya, R. Kumar, A. Krishna, S. Chopra, S. Yadav, G. Moona, M. Jewariya, Single crystal growth of L-tartaric acid and its characterization for optical applications. J. Mater. Sci. Mater. Electron. (2020). https://doi.org/10.1007/s10854-020-02998-4

2. S. Chandran, R. Paulraj, P. Ramasamy, M. Magesh, Crystal growth, vibrational, Hirshfeld surface, thermal, optical, and etching analyses of lithium hydrogen phthalate dehydrate. J. Mater. Sci. Mater. Electron. **31**, 3706–3714 (2020). https://doi.org/10.1007/s10854-020-02929-3

3. V. Sivashankar, R. Siddheswaran, T. Bharthasarathi, P. Murugakoothan, Growth and characterization of new semi organic nonlinear optical zinc guanidinium sulfate single

crystal. J. Cryst. Growth **311**, 2709–2713 (2009). https://doi.org/10.1016/j.jcrysgro.2009.03.001

4. M. Dhavamurthy, R. Raja, K. Syed Suresh Babu, R. Mohan, Crystal structure, growth and characterizations of a novel organic third-order nonlinear optical crystal: guanidinium cinnamate. Appl. Phys. A **122**, 734 (2016). https://doi.org/10.1007/s00339-016-0219-0

5. W. Krumbe, S. Haussuhl, R. Frohlich, Crystal structure and physical properties of monoclinic guanidinium tartrate hydrate. Z. Kristallogr. **187**, 309–318 (1989). https://doi.org/10.1524/zkri.1989.187.14.309

6. T. Arumanayagam, P. Murugakoothan, Studies on optical and mechanical properties of new organic NLO crystal: guanidinium 4-aminobenzoate (GuAB). Mater. Lett. **65**, 2748–2750 (2011). https://doi.org/10.1016/j.matlet.2011.05.081

7. V. Sivashankaran, R. Siddheswaran, P. Murugakoothan, Synthesis, growth, structural, optical and thermal properties of a new semiorganic nonlinear optical guanidinium perchlorate single crystal. Mater. Chem. Phys. **130**, 323–326 (2011). https://doi.org/10.1016/j.matchemphys.2011.06.053

8. Z. Machova, I. Nemec, K. Teubner, P. Nemec, P. Vanek, Z. Micka, The crystal structure, vibrational spectra, thermal behaviour and second harmonic generation of aminoguanidinium (1+) hydrogen L-tartrate monohydrate. J. Mol. Struct. **832**, 101–107 (2007). https://doi.org/10.1016/j.molstruc.2006.08.006

9. R. Frohlich, G. Mattem, Crystal structure of guanidinium fumarate dihydrate. Z. Kristallogr. **172**, 315–317 (1985). https://doi.org/10.1524/zkri.1985.172.14.315

10. P. Karuppasamy, T. Kamalesh, K. Anitha, S. Abdul Kalam, M.S. Pandian, P. Ramasamy, S. Verma, S. Venugopal Rao, Synthesis, crystal growth, structure and characterization of a novel third order nonlinear optical organic single crystal: 2-amino 4,6-dimethyl pyrimidine 4-nitrophenol. J. Opt. Mater. **84**, 475–489 (2018). https://doi.org/10.1016/j.optmat.2018.07.039

11. C.N.R. Rao, *Ultra-Violet and Visible Spectroscopy: Chemical Applications*, 3rd edn. (Butterworths, London, 1975)

12. M. Amudha, R. Rajkumar, V. Thayanithi, P. Praveen Kumar, Growth and characterization of benzimidazolium salicylate: NLO property from a centrosymmetric crystal. Adv. Opt. Technol. **2015**, 1–9 (2015). https://doi.org/10.1155/2015/206325

13. M. Suriya, B. Milton Boaz, K. Sakthi Murugesan, Investigation on the growth, spectral, thermal, mechanical, electrical, laser damage threshold and third-order nonlinear optical studies of 4-acetylanilinium perchlorate (4AAPCl) semi-organic single crystal for optical limiting applications. Appl.

Phys. A **125**, 619 (2019). https://doi.org/10.1007/s00339-019-2905-1

14. S. Karthigha, S. Kalainathan, F. Hamada, M. Yamada, Y. Kondo, Synthesis, growth and third-order nonlinear optical properties of quinolinium single crystal-PCLQI. RSC Adv. **6**, 33159–33169 (2016). https://doi.org/10.1039/C6RA05055G

15. S. Chandran, R. Paulraj, P. Ramasamy, J. Opt. Mater. **52**, 49–55 (2016). https://doi.org/10.1016/j.optmat.2015.11.044

16. K. Senthil, S. Kalainathan, A. Ruban Kumar, P.G. Aravindan, Investigation on synthesis, crystal structure and third-order NLO properties of a new stilbazolium derivative crystal: a promising material for nonlinear optical devices. RSC Adv. (2014). https://doi.org/10.1039/C4RA09112D

17. A. Muthuraja, S. Kalainathan, Study on growth, structural, optical, thermal and mechanical properties of organic single crystal ethyl *p*amino benzoate (EPAB) grown using vertical Bridgman technique. J. Cryst. Growth (2016). https://doi.org/10.1016/j.jcrysgro.2016.11.070

18. N. Sivakumar, N. Kanagathara, G. Bhagavannarayana, S. Kalainathan, G. Anbalagan, Growth, crystalline perfection, optical, thermal, laser damage threshold and electrical characterization of melaminium levulinate monohydrate single crystal. J. Cryst. Growth (2015). https://doi.org/10.1016/j.jcrysgro.2015.05.025

19. S. Vadivel, A.B. Sultan, S.A. Samad, A. Shunmuganarayanan, R. Muthu, Synthesis, structural elucidation, thermal, mechanical, linear and nonlinear optical properties of hydrogen bonded organic single crystal guanidinium propionate for optoelectronic device application. Chem. Phys. Lett. (2018). https://doi.org/10.1016/j.cplett.2018.07.055

20. R. Rajkumar, P. Praveen Kumar, Optical, mechanical, dielectric and thermal properties of piperazinium benzoate single crystal for nonlinear optical applications. J. Opt. (2017). https://doi.org/10.1007/s12596017-0425-y

21. P. Vinothkumar, R. MohanKumar, R. Jayavel, A. Bhaskaran, Synthesis, growth, structural, optical, thermal and mechanical properties of an organic urea maleic acid single crystals for nonlinear optical applications. J. Opt. Laser Technol. **81**, 145–152 (2016). https://doi.org/10.1016/j.optlastec.2016.02.004

22. P. Karuppasamy, M.S. Pandian, P. Ramasamy, S. Verma, Crystal growth, structural, optical, thermal, mechanical, laser damage threshold and electrical properties of triphenylphosphine oxide 4-nitrophenol (TP4N) single crystals for nonlinear optical applications. Opt. Mater. **79**, 152–171 (2018). https://doi.org/10.1016/j.optmat.2018.03.041

23. A. Zamara, K. Rajesh, A. Thirugnanam, P. Praveen Kumar, Growth and characterization of l-histidinium 2-nitrobenzoate [LH2NB(I)]—a promising non linear optical single crystal.

J. Opt. **125**, 6082–6086 (2014). https://doi.org/10.1016/j.ijleo.2014.06.131

24. O. Sahin, O. Uzun, U. Kolemen, B. Duzgun, N. Ucar, Indentation size effect and microhardness study of β-Sn single crystals. Chin. Phys. Lett. **22**, 3137–3140 (2005). https://doi.org/10.1088/0256-307X/22/12/043

25. V. Revathi, V. Rajendran, Investigation about nonlinear optics and antibacterial activity of pyrrolidine-2-carboxylic acid cadmium chloride hydrate single crystal. J. Opt. **154**, 234–241 (2018). https://doi.org/10.1016/j.ijleo.2017.10.060

26. V. Subhashini, S. Ponnusamy, C. Muthamizhchelvan, Synthesis, growth, spectral, thermal, mechanical and optical properties of piperazinium (meso) tartrate crystal: a third order nonlinear optical material. J. Cryst. Growth **363**, 211–219 (2013). https://doi.org/10.1016/j.jcrysgro.2012.10.045

27. M. Sheik-Bahae, A.A. Said, E.W. Van Stryland, High-sensitivity, single-beam n_2 measurements. J. Opt. Lett. **14**, 955–957 (1989). https://doi.org/10.1364/OL.14.000955

28. T. Thilak, M.B. Ahamed, G. Vinitha, Third order nonlinear optical properties of potassium dichromate single crystals by Z-scan technique. J. Opt. **124**, 4716–4720 (2013). https://doi.org/10.1016/j.ijleo.2013.01.111

29. P. Karuppasamy, T. Kamalesh, V. Mohankumar, S. Abdul Kalam, M.S. Pandian, P. Ramasamy, S. Verma, S. Venugopa

Rao, Synthesis, growth, structural, optical, thermal, laser damage threshold and computational perspectives of 4-nitrophenol 4-aminobenzoic acid monohydrate (4NPABA) single crystal. J. Mol. Struct. **1176**, 254–265 (2019). https://doi.org/10.1016/j.molstruc.2018.08.074

30. K. Krishnaraj, N. Sivakumar, P. Praveen Kumar, Growth, spectral, mechanical, electrical and optical characterization of guanidinium hydrogen succinate single crystal. Bull. Mater. Sci. **43**, 41 (2020). https://doi.org/10.1007/s12034-019-2019-6

31. R. Gomathi, S. Madeswaran, D. Rajan Babu, Bulk growth, electrical, linear, third order nonlinear optical and optical limiting properties on bis(cyclohexylammonium) succinate succinic acid crystal. Mater. Chem. Phys. **207**, 84–90 (2018). https://doi.org/10.1016/j.matchemphys.2017.12.051

32. S. Arun Kumar, J. Senthilselvan, G. Vinitha, Third order nonlinearity and optical limiting behaviors of Yb:YAG nanoparticles by Z-scan technique. Opt. Laser Technol. **109**, 561–568 (2019). https://doi.org/10.1016/j.optlastec.2018.08.037

Publisher's Note Springer Nature remains neutral with regard to jurisdictional claims in published maps and institutional affiliations.